The Astrophysical Journal, 766:2 (6pp), 2013 March 20 doi:10.1088/0004-637X/766/1/2

OBSERVATION OF FLUX-TUBE CROSSINGS IN THE SOLAR WIND

L. Arnold[1], G. Li[1], X. Li[1], and Y. Yan[2]
[1] Department of Physics and CSPAR, University of Alabama in Huntsville, Huntsville, AL 35899, USA; gang.li@uah.edu
[2] Key Laboratory of Solar Activity, National Astronomical Observatories of Chinese Academy of Sciences, Beijing 100012, China
Received 2013 January 21; accepted 2013 January 25; published 2013 February 28

ABSTRACT

Current sheets are ubiquitous in the solar wind. They are a major source of the solar wind MHD turbulence intermittency. They may result from nonlinear interactions of the solar wind MHD turbulence or are the boundaries of flux tubes that originate from the solar surface. Some current sheets appear in pairs and are the boundaries of transient structures such as magnetic holes and reconnection exhausts or the edges of pulsed Alfvén waves. For an individual current sheet, discerning whether it is a flux-tube boundary or due to nonlinear interactions or the boundary of a transient structure is difficult. In this work, using data from the *Wind* spacecraft, we identify two three-current-sheet events. Detailed examination of these two events suggests that they are best explained by the flux-tube-crossing scenario. Our study provides convincing evidence supporting the scenario that the solar wind consists of flux tubes where distinct plasmas reside.

Key words: magnetohydrodynamics (MHD) – solar wind – turbulence

Online-only material: animations, color figures

1. INTRODUCTION

The solar wind provides a natural environment in which to study MHD turbulence in a collisionless plasma. Over the past few decades the launches of spacecraft such as *Voyager*, *Helios*, *Ulysses*, *Wind*, and *ACE* have made available a significant amount of data for analyzing the solar wind MHD turbulence.

The first theory of hydrodynamic turbulence, suggested by Kolmogorov (1941), known as the K41 theory, predicted a magnetic field power-law spectrum $\sim k^{-5/3}$. This $-5/3$ exponent arises from the nonlinear interactions of the homogeneous hydrodynamic turbulence in which energy is cascaded from large scales to small scales. For incompressible MHD turbulence where the cascading process is mediated by counterpropagating Alfvén wave packets, the Iroshnikov–Kraichnan (IK) theory (Iroshnikov 1964; Kraichnan 1965) and some recent theories of strong MHD turbulence (Boldyrev 2006; Boldyrev & Perez 2009) predict a power spectrum $\sim k^{-3/2}$.

One important concept in turbulence is intermittency. Ruzmaikin et al. (1995) suggested that intermittent structures can affect the solar wind MHD turbulence power spectrum. They pointed out that the effect of intermittency in the solar wind MHD turbulence is to reduce the exponent of the power-law spectrum. Ruzmaikin et al. (1995, p. 3396) further suggested that intermittency is "in the form of ropes, sheets or more complicated fractal forms." Recently, in studying current sheets in the solar wind, Li et al. (2011) found that the power spectrum of the solar wind magnetic field behaves as K41 in periods that have abundant numbers of current sheets and behaves as IK in periods that are almost current-sheet free (see also Borovsky 2010). Since these current sheets are a source of intermittency, the study of Li et al. (2011) supports Ruzmaikin et al. (1995).

A current sheet is a two-dimensional structure across which the magnetic field direction changes abruptly. Current sheets can be of large scales. For example, the heliospheric current sheet and current sheets found in CME-driven shocks are all large-scale current sheets. These are not the subjects of this study. Here we consider current sheets that are of small scales.

Some current sheets occur in pairs. These can be tangential discontinuities (TDs), often forming the two boundaries of a magnetic hole (see the review of Tsurutani et al. 2011, and references therein), or rotational discontinuities which are the boundaries of an exhaust from a reconnection site (see Gosling et al. 2005 and the review of Gosling 2011). Compared to magnetic holes, reconnection exhausts can be of larger scales. Gosling (2007) has found that the typical width of a reconnection exhaust is $\sim 10^4$ km and some reconnection exhausts can be as wide as 10^5 km. Consequently, these boundaries may be practically identified as a "single-current-sheet" event.

Most current sheets do not occur in pairs. These current sheets can be generated through nonlinear interactions in the MHD turbulence (Zhou et al. 2004; Chang et al. 2004). Using *ACE* data, Vasquez et al. (2007) examined magnetic field discontinuities that can have very small spread angles for Bartels rotation 2286 (day 7 to day 33 in 2001). They found that the statistical properties of these discontinuities form a single population and they are consistent with turbulence generated in situ. By examining the probability density functions (PDFs) of the magnetic field components from a one-dimensional spectral code, Greco et al. (2008) showed that current sheets often occur at the super-Gaussian tail of the PDF. Moreover, Greco et al. (2009) found that, at the inertial scale, in which the energy cascading rate is independent of the scale, the PDF of waiting times (WTs) between MHD discontinuities that are identified in the solar wind using the method of Tsurutani & Smith (1979) and those from MHD simulations are very similar, suggesting that these structures can be explained as a natural result of the nonlinear interaction of the solar wind MHD turbulence.

Other opinions exist. In an earlier work, Bruno et al. (2001) studied current sheets in the solar wind by analyzing *Helios 2* data using the minimum variance method to show how the magnetic field changed over selected time periods. Bruno et al. (2001) were the first to suggest that these structures may be boundaries between flux tubes. Borovsky (2008) analyzed an extended time period of magnetic field from the *ACE* spacecraft and examined the distribution of the spread angle across the current sheets. He showed that the angle distribution has two populations and suggested that the second population, dominating at large angles, could be "magnetic walls" and originate from the surface of the Sun. A solar wind that consists of many flux tubes can be viewed as a structured solar wind.

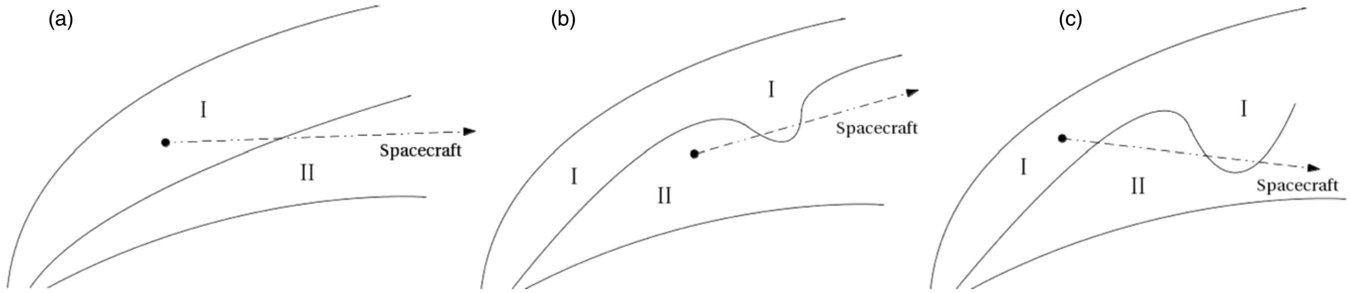

Figure 1. Schematics illustrating (a) a single-current-sheet event, (b) a double-current-sheet event, and (c) a triple-current-sheet event. Note that in the case of a triple-current-sheet event, the spacecraft traverses through two distinct plasmas in the sequence of "I, II, I, II." Consequently, we expect to find the plasma properties to vary accordingly. Dashed line with arrow represents the relative trajectory of the *Wind* spacecraft passing through the flux tubes.

In both the work of Bruno et al. (2001) and Borovsky (2008), the solar wind is envisioned to be full of flux tubes. Observed at a spacecraft, these structures are convected out with the solar wind. A similar scenario where structures convect out from the Sun has been proposed by Tu & Marsch (1991). Analysis on the cross helicity σ_c and residual energy σ_r by Bruno et al. (2007) supported the proposal of Tu & Marsch (1991).

Regardless of the origin of a current sheet, Li (2008) developed a procedure to systematically identify these structures. Using this procedure, Li et al. (2008) examined current sheets in the solar wind and in Earth's magnetotail using *Cluster* magnetic field data and concluded that current sheets are more abundant in the solar wind. Later, Miao et al. (2011) examined over 3 years' worth of slow wind data using *Ulysses* observations and found there were two populations for the distribution of the spread angle across current sheets, in agreement with Borovsky (2008).

Perhaps a large fraction of current sheets identified in the solar wind are due to the nonlinear interactions of the solar wind MHD turbulence, as shown in the work of Greco et al. (2008, 2009). However, a statistical study such as that of Greco et al. (2008, 2009) cannot rule out the possibility that some current sheets in the solar wind are boundaries of flux tubes. Indeed, Borovsky (2008) has used plasma data including proton density and temperature, helium abundance, electron strahl strength, etc. to identify possible plasma boundaries. Plasma data, however, are often of lower time resolution than magnetic field data. Furthermore, plasmas in different flux tubes may have similar properties except different velocities and magnetic field directions. Therefore, to unambiguously separate these two populations can be hard. Note that the occurrence rates of these two populations may have different radial dependence and/or different solar wind type dependence.

In this work, as an effort to identify flux tubes in the solar wind, we present a case study of two "triple-current-sheet" events using data from the *Wind* spacecraft. A triple-current-sheet event is where three current sheets occur in a relatively short period of time. The reason that we want to search for a triple-current-sheet event is as follows. In the flux-tube scenario, the solar wind plasmas reside in different flux tubes and the solar wind magnetic field and plasma properties differ in these flux tubes. Since flux tubes are three-dimensional structures, we expect the boundary between two adjacent flux tubes to be curved and have small-scale ripples. This is shown in the schematics in Figure 1. As these flux tubes are convected out past a spacecraft, depending on the relative configuration of the spacecraft trajectory and these ripples, one expects to observe most often a single crossing as in Figure 1(a), sometimes a double crossing as in Figure 1(b), and occasionally a triple crossing as in Figure 1(c). These three different cases are referred to as "single-current-sheet" events, "double-current-sheet" events, and "triple-current-sheet" events in this study.

A triple-current-sheet event can be used to discriminate between the scenario where current sheets are generated in situ and the scenario where current sheets originate from the surface of the Sun. In the former case, one expects no correlations between these current sheets in the sense that plasmas before and after these current-sheet crossings need not show any relationships. In the latter case, however, the spacecraft traverses through two distinct plasmas in the sequence of "I, II, I, II," so the observed plasma properties do not vary arbitrarily.

2. DATA SELECTION AND ANALYSIS

We use the 3 s plasma and magnetic field data from the 3DP (Lin et al. 1995) and magnetic field (Lepping et al. 1995) experiments on the *Wind* spacecraft. The data period was from 1995 September to October, which was during the declining phase of the solar cycle. It is ideal to select data in the solar minimum period due to a lack of transient structures such as CMEs. For the data analysis method of current-sheet identification, the readers are referred to Li (2008) and Miao et al. (2011).

In the following, we first present a single-current-sheet event and a double-current-sheet event. We then present two triple-current-sheet events.

Figure 2 is a single-current-sheet event that occurred on 1995 September 21. The current sheet in Figure 2 is located at 14:32 UT and is shown by the brown vertical line. Before the current sheet, the magnetic field magnitude $|B|$ decreases and the proton density N_p increases. In the scenario where a current sheet is the boundary of a flux tube, these changes across the current sheet occur because plasmas in different flux tubes have different properties (as shown in panel (a) of Figure 1). However, one need not invoke the flux-tube-crossing scenario to explain Figure 2. It can be simply a TD or one side of a reconnection exhaust. Indeed, careful examination shows that there was another small current sheet on ∼14:32 UT, when $|B|$ decreased and N_p increased. Our selection procedure did not pick out this earlier current sheet.

The change across the current sheets is Alfvénic. The angle between $\delta \boldsymbol{B}$ and $\delta \boldsymbol{V}$ across the current sheet is 7°. For the earlier current sheet (which did not get picked up by our procedure), the angle is 173°. Such parallel and anti-parallel Alfvénic changes are always associated with a reconnection exhaust (Gosling 2011). Furthermore, there was also a decrease of magnetic field and an increase of number density (but not temperature) between these two current sheets, providing another support for identification of a reconnection exhaust. Therefore, Figure 2,

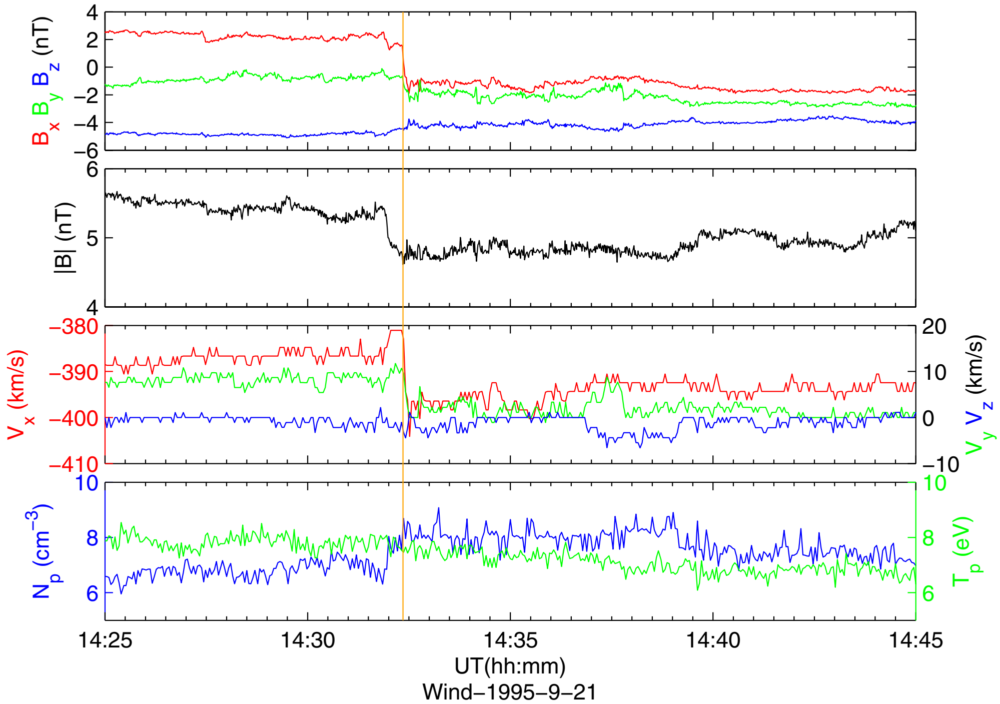

Figure 2. Single-current-sheet event that occurred on 1995 September 21. Shown from top to bottom are the three components of the vector magnetic field in the Geocentric Solar Ecliptic (GSE) coordinate system, the magnitude of the magnetic field, the three components of the vector proton velocity in the GSE coordinate system, and the solar wind proton number density and proton temperature, respectively. The brown vertical line marks the location of the current sheet.

(A color version of this figure is available in the online journal.)

although identified as a single-current-sheet event using the Li (2008) algorithm, is really part of a pair of a bifurcated current sheet (Gosling et al. 2005; Gosling 2007, 2011).

Figure 3 is a double-current-sheet event. Two current sheets can be identified around 11:11:48 UT and 11:12:26 UT. In the scenario of flux-tube crossing, Figure 3 can be understood as the spacecraft briefly crosses the magnetic wall between two flux tubes and then returns to the original flux tube. The schematic of this event is shown in the second panel of Figure 1. Note that the temperature decreases and the proton density increases between the two current sheets. As in Figure 2, although Figure 3 can be explained by the flux-tube-crossing scenario, it need not be. The angles between δB and δV across the two current sheets are 175° and 167°. Unlike the first event, this double current sheet is not associated with a reconnection exhaust. There was a slight but insignificant drop in the magnetic field magnitude, so it is unlikely to be a magnetic hole. The proton number density and proton temperature were also changed slightly at the two current sheets. These slight changes, together with the pulse-like changes of the three magnetic field components, suggest that this structure could be a pulsed Alfvén wave (Gosling et al. 2011, 2012). Note, if this was a pulsed Alfvén wave, then according to Figure 3(a) of Gosling et al. (2012) and the fact that it has a duration of 46 s, it would be a long-duration pulsed Alfvén wave.

Figures 4 and 5 show two triple-current-sheet events that occurred on 1995 October 2 and 1995 October 13, respectively. Consider first the event shown in Figure 4. Throughout the event both B_y and V_y did not change much. B_x underwent a sharp change at 22:13:05 UT, the first current sheet, after which it only changed slightly, until 22:25:00 UT when another sharp change occurred and B_x returned to values similar to those before 22:13:00 UT. At 22:25:00 UT at the third current sheet another sharp change in B_x occurred. After the crossing B_x at and after 22:25:32 UT returned to a value comparable to B_x at 22:24:30 UT, just before crossing the second current sheet. From the third panel, we can see that the V_x changes at the same times as B_x.

Similar behavior also occurred with B_z and V_z. Before crossing the first current sheet at 22:13:05 UT, B_z (V_z) was almost a constant. After the crossing, B_Z increased and V_z decreased. B_z also became slightly more turbulent. At the second crossing at 22:25:00 UT, B_z and V_z changed back to almost the same value as before 22:13:00 UT. Then both B_z and V_z underwent another sudden change at the third current sheet crossing at 22:25:30 UT. After the third crossing, B_z returned to a value similar to that before the second crossing at 22:25:00 UT.

The magnitude of the magnetic field $|B|$ (the second panel), the proton number density N_p and the proton temperature T_p (the fourth panel) did not vary much throughout the event. Before the crossing of the second current sheet, around 22:24:30 UT, $|B|$ increased and N_P and T_p decreased. To better illustrate how the magnetic field direction evolves in this event, we have constructed an animation of the evolution of the unit magnetic field $\hat{B}$.

There are two facts worth noting. (1) Various plasma properties, including N_p, T_p, and the three components of $\boldsymbol{B}$ and $\boldsymbol{V}$ in the short period between 22:25:00 UT and 22:25:30 UT are very similar to those prior to 22:13:00 UT, suggesting that these are the same solar wind plasma. This can be clearly seen in the online animation. (2) Similarly, the solar wind before and after the short period is likely the same and it is different from that in (1).

One may attempt to explain this triple-current-sheet event as the spacecraft crossing three uncorrelated individual current sheets that are generated by independent nonlinear interactions

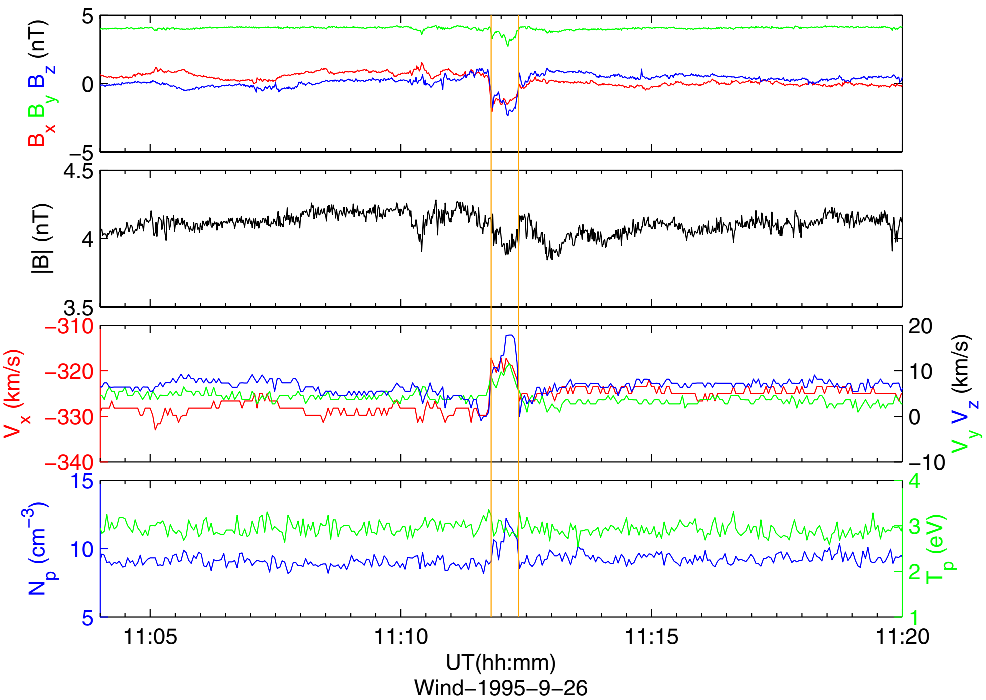

Figure 3. Double-current-sheet event that occurred in 1995 September 26. Shown from top to bottom are the three components of the vector magnetic field in the Geocentric Solar Ecliptic (GSE) coordinate system, the magnitude of magnetic field, the three components of the vector proton velocity in the GSE coordinate system, and the solar wind proton number density and proton temperature, respectively. The two brown vertical lines mark the location of the current sheet.

(A color version of this figure is available in the online journal.)

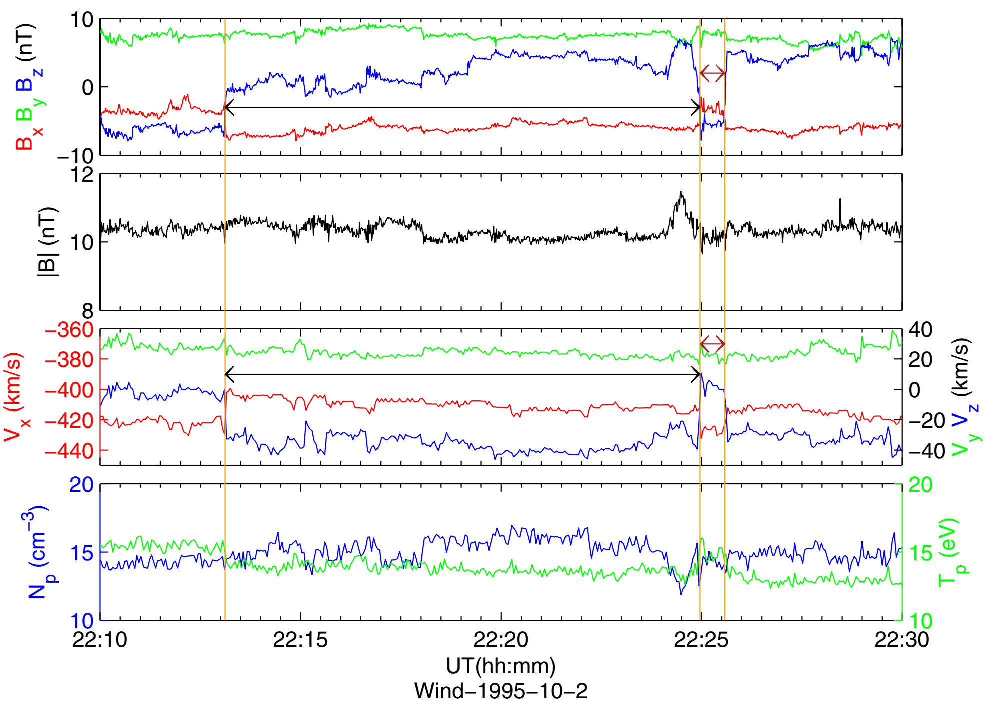

Figure 4. Triple-current-sheet event occurred that on 1995 October 2. Shown from top to bottom are the three components of the vector magnetic field in the Geocentric Solar Ecliptic (GSE) coordinate system, the magnitude of magnetic field, the three components of the vector proton velocity in the GSE coordinate system, and the solar wind proton number density and proton temperature, respectively. The three vertical lines mark the location of the current sheet. Also see the online animation of the evolution of the unit magnetic field $\hat{B}$ in this event.

(An animation and a color version of this figure are available in the online journal.)

of the solar wind MHD turbulence. However, since independent current sheets have no correlations, the chance of the solar wind returning back to its original state after two independent current sheet crossings would be minute. Alternatively, one may argue that the plasma between 22:13:05 UT and 22:25:00 UT represented a rather long-lived transient structure, and one could interpret the first two current sheets as the boundaries of this structure. In such a case, one has to explain why, after the

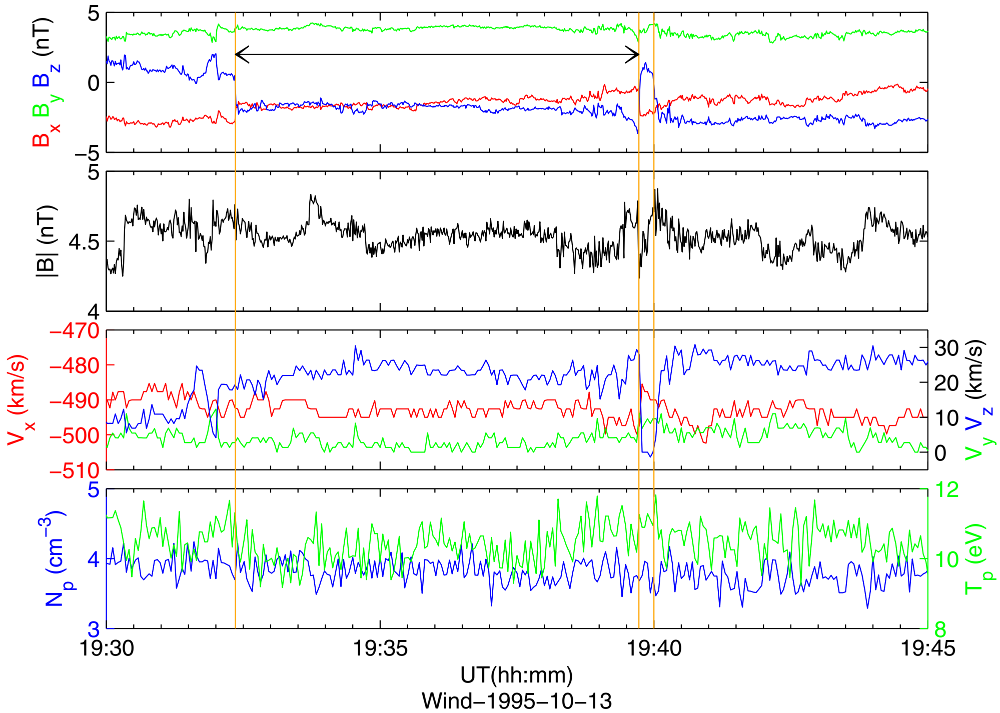

Figure 5. Same as Figure 4, but for the 1995 October 13 event. Shown from top to bottom are the three components of the vector magnetic field in the Geocentric Solar Ecliptic (GSE) coordinate system, the magnitude of magnetic field, the three components of the vector proton velocity in the GSE coordinate system, and the solar wind proton number density and proton temperature, respectively. The three vertical lines mark the location of the current sheet. Also see the online animation of the evolution of the unit magnetic field $\hat{B}$ in this event.

(An animation and a color version of this figure are available in the online journal.)

third-current-sheet crossing, both the magnetic field and the plasma return to values the same as inside the transient structure.

Another triple-current-sheet event is the 1995 October 13 event, which is shown in Figure 5. Unlike in the 1995 October 2 event, the three components of $\boldsymbol{B}$ and $\boldsymbol{V}$, in particular, B_x and V_x, suffered some additional changes at and around the three current sheets, making the 1995 October 13 event less convincing than the 1995 October 2 event.

The first current sheet is located at 19:32:28 UT. Both B_x and B_z showed a sudden jump across the first current sheet; V_x and V_z did not show significant changes. B_y and V_y also did not vary across the first current sheet. The current sheet is therefore non-Alfvénic. After crossing the first current sheet, B_z was almost a constant for the next ∼7 minutes until 19:39:40 UT, where the second current sheet was encountered. It increased across the second current sheet to a value similar to those prior to the crossing of the first current sheet. Compared to B_z, B_x was nearly constant after crossing the first current sheet for ∼3 minutes and then gradually increased until 19:39:00 UT, after which it increased noticeably before the second current sheet. Across the second current sheet, it dropped to a value similar to those prior to the crossing of the first current sheet. The third current sheet occurred at 19:40:15 UT. Across the third current sheet, there was a significant change of B_z and a small change of B_x. The two black horizontal dashed lines indicate that B_x (B_z) before the first current sheet was similar to B_x (B_z) between the second and the third current sheets. The two magenta horizontal dashed lines indicate that B_x (B_z) between the first and the second current sheets was similar to B_x (B_z) after the third current sheet. Note that the change of B_x at the third current sheet was smaller than that at the second current sheet. After the third current sheet, B_x kept increasing, until 19:40:30 UT. The value of B_x after 19:40:30 UT is similar to those before 19:39:00 UT. As in the 1995 October 2 event, we also constructed an animation of the evolution of the unit magnetic field $\hat{B}$ for this event.

For the 1995 October 2 event, the angles between δB and δV across the three current sheets are 179°, 176°, and 174°, respectively. For the 1995 October 13 event, the angles between δB and δV are 155°, 124°, and 173°, respectively. While the three current sheets in the 1995 October 2 event are highly Alfvénic, those in the 1995 October 13 event are not.

3. DISCUSSION AND SUMMARY

Current sheets are ubiquitous in the solar wind. They can be generated in situ through nonlinear interactions of the solar wind MHD turbulence (Greco et al. 2008, 2009), or represent the boundaries of flux tubes that originated at the Sun (Bruno et al. 2001; Borovsky 2008; Li et al. 2008). Appearing in pairs, they could also be the boundaries of reconnection exhausts (Gosling 2011).

An intriguing question one may ask is: For any particular current sheet, can we identify how it originated?

If current sheets that are generated in situ and those that are convected out from the Sun have similar properties (such as the spread angles, the current-sheet width, etc.), then discriminating between these two scenarios can be hard. However, as shown in the rightmost schematic in Figure 1, the presence of a triple-current-sheet event provides strong support to the flux-tube scenario. This is because in the flux-tube scenario the plasma and field changes across the three current sheets are intimately correlated: as the spacecraft crosses the three current sheets, the plasma before the first crossing and that between the second and the third crossing are the same; the plasma between the first and the second crossings and that after the third are the same. This is in stark contrast to the scenario where the current sheets are generated in situ. In the latter scenario, the plasma changes at the three current sheets in a triple-current-sheet event need not match.

Note that the identification of a triple-current-sheet event does not tell us how many single-current-sheet events are due to flux-tube crossing. As discussed earlier, since a reconnection exhaust can be of large scale (Gosling 2007), some single-current-sheet events we identify can be the boundaries of reconnection exhausts. Gosling (2010) identified an occurrence rate of 40–80 reconnection events per month in solar minimum. In our study, we only consider current sheets that are abrupt (width <10 s) and whose spread angles are larger than 45°; we find about 350 "single-current-sheet" events per month. Assuming that $2 * 60 = 120$ are boundaries of reconnection exhausts, then the rest are presumably either generated in situ or are the boundaries of flux tubes. Assuming that 80% (50%) of the rest are generated in situ, then one gets about 45 (115) single-current-sheet events that are flux-tube crossings per month.

If current sheets are boundaries of flux tubes that have a solar origin, e.g., super granules, then one may expect to find some statistical correlations between in situ observations of current sheets and solar observation of super granules. Indeed, Bruno et al. (2001) have suggested that the sizes of the flux tubes, when tracing back to the solar surface, may correlate with the size of photospheric magnetic networks. In the work of Miao et al. (2011), using *Ulysses* observations, the distribution of the WT statistics of the current sheets was obtained. Assuming that these flux tubes do not split or merge during their propagation to 1 AU, then one may expect such WT statistics resemble the distribution of the magnetic network sizes. Examining the WT statistics of a current sheet, and in particular, its dependence on heliocentric distance, and its correlation with supergranule size will be reported in future work.

To conclude, we have examined two months' worth of solar wind data from the *Wind* spacecraft and identified two triple-current-sheet events. The sequence of the observed magnetic field and plasma data in these two events is in agreement with the scenario where current sheets are flux-tube boundaries, as depicted in Figure 1. Unambiguous identification of flux tubes in the solar wind is important because these structures present an additional source of solar wind MHD turbulence intermittency. They can affect the power spectrum of the solar wind MHD turbulence (Li et al. 2011, 2012) as well as affecting the transport of energetic particles in the solar wind (Qin & Li 2008).

We thank R. P. Lepping and R. P. Lin and the CDAWeb for making available the data used in this paper and the referee for very valuable suggestions. This work is supported in part by NSF grants ATM-0847719, AGS0962658, AGS1135432 and NASA grants NNH07ZDA001N-HGI and NNX07AL52A.

REFERENCES

Boldyrev, S. 2006, PhRvL, 96, 115002
Boldyrev, S., & Perez, J. 2009, PhRvL, 103, 225001
Borovsky, J. E. 2008, JGRA, 113, A08110
Borovsky, J. E. 2010, PhRvL, 105, 111102
Bruno, R., Carbone, V., Veltri, P., Pietropaolo, E., & Bavassano, B. 2001, P&SS, 49, 1201
Bruno, R., D'Amicis, R., Bavassano, B., Carbone, V., & Sorriso-Valvo, L. 2007, AnG, 25, 1913
Chang, T., Tam, S., & Wu, C. 2004, PhPl, 11, 1287
Gosling, J. T., Skoug, R. M., McComas, D. J., & Smith, C. W. 2005, JGR, 110, A01107
Gosling, J. T. 2007, ApJL, 671, L73
Gosling, J. T. 2010, in AIP Conf. Proc. 1216, 12th Solar Wind Conference, ed. M. Maksimovic, K. Issautier, N. Meyer-Vernet et al. (Melville, NY: AIP), 188
Gosling, J. T. 2011, SSRv, 172, 187
Gosling, J. T., Tian, H., & Phan, T. D. 2011, ApJL, 737, L35
Gosling, J. T., Tian, H., & Phan, T. D. 2012, ApJL, 751, L22
Greco, A., Chuychai, P., Matthaeus, W. H., Servidio, S., & Dmitruk, P. 2008, GeoRL, 35, L19111
Greco, A., Matthaeus, W. H., Servidio, S., Chuychai, P., & Dmitruk, P. 2009, ApJL, 691, L111
Iroshnikov, P. S. 1964, SvA, 7, 566
Kolmogorov, A. 1941, C. R. Acad. Sci. URSS, 30, 301
Kraichnan, R. H. 1965, PhFl, 8, 1385
Lepping, R. L., Acũna, M. H., Burlaga, L. F., et al. 1995, SSRv, 71, 207
Li, G. 2008, ApJL, 672, L65
Li, G., Lee, E., & Parks, G. 2008, AnG, 26, 1889
Li, G., Miao, B., Hu, Q., & Qin, G. 2011, PhRvL, 106, 125001
Li, G., Qin, G., Hu, Q., & Miao, B. 2012, AdSpR, 49, 1327
Lin, R. P., Anderson, K. A., Ashford, S., et al. 1995, SSRv, 71, 125
Miao, B., Peng, B., & Li, G. 2011, AnGeo, 29, 237
Qin, G., & Li, G. 2008, ApJ, 682, L129
Ruzmaikin, A., Feynman, J., Goldstein, B., Smith, E., & Balogh, A. 1995, JGRA, 100, 3395
Tsurutani, B. T., Lakhina, G. S., Verkhoglyadova, O. P., et al. 2011, JGR, 116, A02103
Tsurutani, B. T., & Smith, E. J. 1979, JGR, 84, 2773
Tu, C.-Y., & Marsch, E. 1991, AnG, 9, 319
Vasquez, B. J., Abramenko, V. I., Haggerty, D. K., & Smith, C. W. 2007, JGR, 112, A11102
Zhou, Y., Matthaeus, W., & Dmitruk, P. 2004, RvMP, 76, 1015